



3 4456 0003988 4

ORNL/TM-9653

ornl

**OAK RIDGE
NATIONAL
LABORATORY**

MARTIN MARIETTA

The Poloidal Potential in the Low-Collisionality Regime in a Nonaxisymmetric Torus

D. E. Hastings
J. S. Tolliver

OAK RIDGE NATIONAL LABORATORY

CENTRAL RESEARCH LIBRARY

CIRCULATION SECTION

430N SOUTH ST.

LIBRARY LOAN COPY

DO NOT TRANSFER TO ANOTHER PERSON

If you wish someone else to see this
report, send in name with report and
the library will arrange a loan.

OPERATED BY
MARTIN MARIETTA ENERGY SYSTEMS, INC.
FOR THE UNITED STATES
DEPARTMENT OF ENERGY

Printed in the United States of America. Available from
National Technical Information Service
U.S. Department of Commerce
5285 Port Royal Road, Springfield, Virginia 22161
NTIS price codes—Printed Copy: A03; Microfiche A01

This report was prepared as an account of work sponsored by an agency of the United States Government. Neither the United States Government nor any agency thereof, nor any of their employees, makes any warranty, express or implied, or assumes any legal liability or responsibility for the accuracy, completeness, or usefulness of any information, apparatus, product, or process disclosed, or represents that its use would not infringe privately owned rights. Reference herein to any specific commercial product, process, or service by trade name, trademark, manufacturer, or otherwise, does not necessarily constitute or imply its endorsement, recommendation, or favoring by the United States Government or any agency thereof. The views and opinions of authors expressed herein do not necessarily state or reflect those of the United States Government or any agency thereof.

ORNL/TM-9653

Dist. Category UC-20 g

Fusion Energy Division

THE POLOIDAL POTENTIAL IN THE LOW-COLLISIONALITY
REGIME IN A NONAXISYMMETRIC TORUS

D. E. Hastings

J. S. Tolliver

Computing and Telecommunications Division
Martin Marietta Energy Systems, Inc.

Date Published: January 1986

Prepared by the
OAK RIDGE NATIONAL LABORATORY
Oak Ridge, Tennessee 37831
operated by
MARTIN MARIETTA ENERGY SYSTEMS, INC.
for the
U.S. DEPARTMENT OF ENERGY
under Contract No. DE-AC05-84OR21400



3 4456 0003988 4

CONTENTS

| | |
|---|----|
| ABSTRACT..... | v |
| I. INTRODUCTION..... | 1 |
| II. THE POLOIDAL ELECTRIC FIELD: BASIC PRINCIPLES..... | 3 |
| III. DERIVATION OF EQUATIONS FOR THE POLOIDAL ELECTRIC FIELD..... | 7 |
| IV. DESCRIPTION OF THE NUMERICAL METHOD..... | 18 |
| V. NUMERICAL RESULTS..... | 20 |
| VI. CONCLUSIONS..... | 26 |
| ACKNOWLEDGMENTS..... | 27 |
| REFERENCES..... | 28 |

ABSTRACT

The poloidal potential is calculated numerically in the low-collisionality regime for nonaxisymmetric tori such as stellarators and bumpy tori. It is found that even fairly deep into the superbanana regime, the poloidal potential retains the simple azimuthal dependence of the plateau regime.

I. INTRODUCTION

In the pioneering work of Hinton and Rosenbluth,¹ it was shown that the self-consistent poloidal potential in a single-ion plasma in a tokamak was insignificant in its effect on transport compared to the magnetic-gradient-induced transport. This occurs because the self-consistent potential is small both in the inverse aspect ratio and in the ratio of the poloidal ion gyroradius to the temperature length scale. After this work Hazeltine and Ware² showed that in an impure tokamak plasma the poloidal potential could be substantial. This occurs because the plasma parallel flow can be of the same order as the impurity thermal velocity, leading to a significant viscosity that drives electrostatic variation on the flux surface. Since then several authors have explored the effect of a significant poloidal potential on neoclassical transport.^{3,4} Generally, it is found that the electrostatic potential can make a factor of two or more enhancement in the transport coefficients, when its magnitude is the same order as the magnetic field inhomogeneity.

The poloidal potential has also been calculated in other confinement devices such as bumpy tori,⁵ tandem mirrors,⁶ and stellarators.⁷ In these devices the poloidal potential can significantly modify the neoclassical transport rates. It has also been shown that in a bumpy torus⁸ island structures can form in the poloidal potential that have a large amount of convective loss associated with them.

All of these works in nonaxisymmetric geometries have calculated the poloidal potential in the resonant plateau regime or the large electric field nonresonant regime. In these regimes the potential can

be obtained analytically because the particle orbits can be expressed very simply or the effect of collisions makes the orbit details unimportant. The regimes that have not been addressed in the literature of the poloidal electric field in nonaxisymmetric devices are the resonant banana regime in a tandem mirror and the superbanana regime in a stellarator or bumpy torus. These regimes are not accessible analytically because the orbits are very complicated and collisions are too weak to smear out the details of the orbits.

In this paper we shall address the question of the poloidal electric field in the superbanana regime, in a stellarator or a bumpy torus. In Sec. II we shall review the physics behind the calculation of the poloidal potential and consider it from two different points of view. In Sec. III we derive the equation and boundary conditions for the kinetic equation, describing the distribution function in the superbanana regime. We also show the similarity to the results of Hinton and Rosenbluth in Ref. 1. In Sec. IV we describe the numerical method used to solve the equations for the distribution function and for the potential. In Sec. V we present the numerical results, which indicate that for a tokamak the poloidal potential takes on a complicated azimuthal dependence for low collisionalities, but for a stellarator or bumpy torus the poloidal potential takes a very simple form. This is true despite the complicated orbit structure in the superbanana regime. Finally, in Sec. VI, we indicate where future areas of research could lie in this important question of the structure of the poloidal electric field.

II. THE POLOIDAL ELECTRIC FIELD: BASIC PRINCIPLES

In this section we shall review the basic ideas behind the calculation of the poloidal electric field. First, we consider the Eulerian approach adopted in Ref. 1.

The lowest order distribution function in the expansion parameter $\Delta r/r_n$ (where Δr is the orbit deviation from a flux surface and r_n is a typical macroscopic length scale in the plasma) is taken to be a Maxwellian,

$$f_0 = N \left(\frac{m}{2\pi T} \right)^{3/2} e^{-E/T}, \quad (1)$$

where the subscript on f indicates order in $\Delta r/r_n$ and N is a normalization factor. The energy E is defined by

$$E = \frac{1}{2} m v^2 + Ze\phi, \quad (2)$$

where $\phi(\alpha, \beta)$ is the potential, which is a function of the radial flux variable α and the poloidal variable β . We define the flux surface average $\langle \dots \rangle$ of any function G by

$$\langle G \rangle = \frac{1}{\int d\beta \int dl/B} \int d\beta \int \frac{dl}{B} G \quad (3)$$

and define the poloidal potential $\tilde{\phi}$ by

$$\tilde{\phi} = \phi - \langle \phi \rangle. \quad (4)$$

The lowest order number density n_0 is

$$n_0 = \int d^3v f_0 = Ne^{-\frac{Ze\langle\Phi\rangle}{T}} e^{-\frac{Ze\tilde{\Phi}}{T}}, \quad (5)$$

while the flux surface average density is

$$\langle n_0 \rangle = Ne^{-\frac{Ze\langle\Phi\rangle}{T}} \langle e^{-\frac{Ze\tilde{\Phi}}{T}} \rangle ;$$

hence, from Eq. (5) n_0 can be written in terms of its flux surface average by

$$n_0 = \langle n_0 \rangle \frac{e^{-\frac{Ze}{T} \tilde{\Phi}}}{\langle e^{-\frac{Ze}{T} \tilde{\Phi}} \rangle}. \quad (6)$$

From Eq. (6) we see that the lowest order number density and the flux surface average density do not coincide, precisely because of the existence of a poloidal potential. If we have $Ze\tilde{\Phi}/T \ll 1$, then

$$n_0 \approx \langle n_0 \rangle \left(1 - \frac{Ze}{T} \tilde{\Phi} \right). \quad (7)$$

Physically the plasma behaves as a fluid and tends to form constant density contours on the constant potential contours, which in the presence of a poloidal potential are offset from the flux surfaces.

The first-order density perturbation arises from the motion of guiding centers off the flux surface and is

$$n_1 = \int d^3v f_1. \quad (8)$$

The plasma must remain quasi neutral so that through first order in $\Delta r/r_n$ we have

$$\sum_a Z_a \left[\langle n_{0a} \rangle \left(1 - \frac{Z_a e}{T_a} \tilde{\Phi} \right) + \int d^3v f_{1a} \right] = 0 . \quad (9)$$

To lowest order $\sum_a Z_a \langle n_{0a} \rangle = 0$; hence, we have a relationship for $\tilde{\Phi}$,

$$\tilde{\Phi} \sum_a \frac{Z_a^2 e}{T_a} \langle n_{0a} \rangle = \sum_a Z_a \int d^3v f_{1a} . \quad (10)$$

In general, this is a nonlinear differential system because the first-order distribution function can depend in a complex fashion on $\tilde{\Phi}$. From this expression it is clear that the guiding center drifts off the flux surface are responsible for forming the poloidal potential.

An alternative way of looking at the poloidal potential is the Lagrangian formulation in the space of the constants of the motion.⁹ We take three constants of the motion $\underline{J} = (J_1, J_2, J_3)$, where J_1 and J_2 describe velocity space while J_3 describes the radial direction in configuration space. In these variables the lowest order distribution function f_0 (in $\Delta J_3/J_3$) is given by

$$f_0 = \frac{n_3(J_3)}{(2\pi m T)^{3/2}} \frac{dJ_3}{dv} e^{-E/T + Ze\Phi/T} , \quad (11)$$

where

$$J_3 = 2\pi Ze\alpha + \Delta J_3 , \quad (12)$$

and n_3 is defined by

$$n_3(J_3) = \int d^3\underline{J} d^3\underline{\theta} \delta[\underline{x} - \underline{x}(\underline{J}, \underline{\theta})] f, \quad (13)$$

where the angles $\underline{\theta}$ are the conjugate angles to the constants of the motion \underline{J} . From Ref. 9 we obtain

$$n_0 = n_3 \frac{dJ_3}{dv} + Ze \int dJ_1 dJ_2 \frac{B\omega_2}{|v_{\parallel}|} \Delta J_3 \frac{\partial f_0}{\partial J_3}. \quad (14)$$

The first term in Eq. (14) is the flux surface average density, so once again we see that the lowest order density is the flux surface average density plus an explicit contribution, which arises from the fact that the distribution function tries to be constant on contours of constant J_3 . Here, however, we can clearly see that this correction to n_0 is driven by the orbit deviation ΔJ_3 . The first-order quasi-neutrality relationship can be written

$$\sum_a Z_a \int dJ_1 dJ_2 \frac{B\omega_2}{|v_{\parallel}|} Z_a e \left[\Delta J_3 \frac{\partial f_{0a}}{\partial J_3} + f_{1a} \right] = 0. \quad (15)$$

If we define the orbit average $\langle \alpha \rangle_0$ by $J_3 = 2\pi Ze \langle \alpha \rangle_0$, then using Eq. (12) we obtain $\Delta J_3 = -2\pi Ze(\alpha - \langle \alpha \rangle_0)$. The quasi-neutrality relationship in Eq. (15) can then be transformed to

$$\sum_a Z_a \int d^3v \left[-(\alpha - \langle \alpha \rangle_0) \frac{\partial f_0}{\partial \alpha} + f_1 \right] = 0. \quad (16)$$

If to lowest order in collisionality f_1 can be written as $f_1 = -(\alpha - \langle \alpha \rangle_0) \partial f_0 / \partial \alpha$, as is true in a bumpy torus,⁵ then Eq. (16) becomes

$$\sum_a Z_a \int d^3v \left[-2(\alpha - \langle \alpha \rangle_0) \frac{\partial f_0}{\partial \alpha} \right] = 0 .$$

Now we can see clearly that if $\alpha - \langle \alpha \rangle_0$ is independent of velocity space variables (which is true if the orbit deviation is caused only by $\underline{E} \times \underline{B}$ drifts), then we have

$$\sum_a Z_a \int d^3v \left[-2(\alpha - \langle \alpha \rangle_0) \frac{\partial f_0}{\partial \alpha} \right] = -2(\alpha - \langle \alpha \rangle_0) \frac{\partial}{\partial \alpha} \sum_a Z_a \langle n_{0a} \rangle = 0 .$$

Hence, quasi neutrality is automatically satisfied through first order if we have only $\underline{E} \times \underline{B}$ drifts off the flux surface. This then implies that in order for a poloidal potential to exist, we must have drifts that have velocity space structure like $\underline{v}B$ drifts.

III. DERIVATION OF EQUATIONS FOR THE POLOIDAL ELECTRIC FIELD

In Eq. (10) we have the equation for $\tilde{\phi}$ in terms of f_{1a} . To complete this equation we need to determine f_{1a} in terms of $\tilde{\phi}$. We will work in the low-collisionality superbanana regime in a stellarator and a bumpy torus.

The model for the magnetic field is taken to be

$$\frac{B}{B_0} = 1 - \epsilon_t \cos \theta - \epsilon_h(r) \cos(l\theta - m\phi) , \quad (17)$$

where the radial variable "r" is defined by $\alpha = \frac{1}{2}r^2B_0$, the azimuthal angle θ is $\theta = \beta$, ϵ_t is the inverse aspect ratio r/R_0 , ϵ_h is the helical modulation of the field, ϕ is the toroidal angle, and l and m are the poloidal and toroidal winding numbers. Note that for a bumpy torus we have $l = 0$.

The linearized bounce-averaged drift kinetic equation for f_{1a} is

$$\langle \dot{r} \rangle_b \frac{\partial f_{1a}}{\partial r} + \langle \dot{r} \rangle_b \frac{\partial F_{Ma}}{\partial r} + \langle \dot{\theta} \rangle_b \frac{\partial f_{1a}}{\partial \theta} = \frac{1}{\tau_b} \oint \frac{dl}{v_{\parallel}} C(f_{1a}), \quad (18)$$

where $\tau_b = \oint dl/v_{\parallel}$ is the bounce time in a helical well and the bounce-averaged drift $\langle \dot{\theta} \rangle_b$ is

$$\langle \dot{\theta} \rangle_b = \frac{1}{rB_0} \frac{\partial \langle \Phi \rangle}{\partial r} + \frac{\mu B_0}{ZerB_0} \left\{ \epsilon_h \left[\frac{2E(k)}{K(k)} - 1 \right] + \epsilon_t' \right\}. \quad (19)$$

The prime (') means $\partial/\partial r$, and K and E are the complete elliptic integrals of the first and second kind with argument k , which is given by $k^2 = \left[E - Ze\langle \Phi \rangle - \mu B_0(1 - \epsilon_t - \epsilon_h) \right] / (2\mu B_0 \epsilon_h)$. Particles are helically trapped for $0 \leq k < 1$ and untrapped for $k > 1$. The bounce-averaged radial drift $\langle \dot{r} \rangle_b$ is

$$\langle \dot{r} \rangle_b = - \frac{\mu B_0}{ZerB_0} \epsilon_t \sin \theta - \frac{1}{rB_0} \frac{\partial \tilde{\Phi}}{\partial \theta}. \quad (20)$$

The poloidal potential makes a contribution to $\langle \dot{r} \rangle_b$ through the radial $\underline{E} \times \underline{B}$ drift associated with it.

In the superbanana regime the dominant contribution to the distribution function comes from resonant particles with $\langle \dot{\theta} \rangle_b = 0$ somewhere along their orbits. For these particles the collision operator can be approximated by

$$\frac{1}{\tau_b} \oint \frac{dl}{v_{\parallel}} C(f_1) \approx v_c(w) \Omega_{th}^2 \frac{\partial^2 f_1}{\partial \langle \dot{\theta} \rangle_b^2}, \quad (21)$$

where $v_c(w)$ is the collision frequency evaluated along the resonance curve $\langle \dot{\theta} \rangle_b = 0$ in the (w, μ) space with w being the kinetic energy. The frequency Ω_{th} is the ∇B drift evaluated at the thermal velocity, $\Omega_{th} = (T/ZerB_0)\epsilon_h$. If r_0 is the flux surface on which $\langle \dot{\theta} \rangle_b = 0$, then we can transform the kinetic equation [Eq. (19)], using Eq. (21), to the form

$$\begin{aligned} \frac{\partial^2 f_1}{\partial z^2} - z \frac{\partial f_1}{\partial \theta} - \left[\frac{\Omega_{th}}{v_c(w)} \right]^{2/3} \frac{\Omega'_0}{\Omega_{th}^2} \langle \dot{r} \rangle_b \frac{\partial f_1}{\partial z} \\ = \langle \dot{r} \rangle_b \frac{1}{\Omega_{th}} \left(\frac{v_c(w)}{\Omega_{th}} \right)^{-1/3} \frac{\partial F_M}{\partial r}. \end{aligned} \quad (22)$$

The details of this transformation can be found in Ref. 10. In Eq. (22) z is a boundary layer variable defined by $z = [\Omega_{th}/v_c(w)]^{1/3} \langle \dot{\theta} \rangle_b / \Omega_{th}$, $\Omega'_0 = \partial / \partial r (\langle \dot{\theta} \rangle_b)_{r=r_0}$ and evaluated along the resonance curve $\langle \dot{\theta} \rangle_b = 0$.

We can simplify Eq. (22) by taking $\mu B_0 \approx w$ in $\langle \dot{r} \rangle_b$, defining a dimensionless poloidal potential by

$$\hat{\phi} = \frac{e}{T} \tilde{\phi} \frac{1}{\epsilon_t}, \quad (23)$$

and defining a parameter $y(w)$ by

$$y(w) = \left(\frac{\Omega_{th}}{v_c(w)} \right)^{2/3} \frac{\Omega_0'}{\Omega_{th}^2} \left[- \frac{w}{ZerB_0} \epsilon_t \right] ; \quad (24)$$

then the kinetic equation becomes

$$\frac{\partial^2 \hat{f}}{\partial z^2} - z \frac{\partial \hat{f}}{\partial \theta} - y(w) \left[\sin \theta + \left(\frac{T}{w} \right) \frac{\partial \hat{\Phi}}{\partial \theta} \right] \frac{\partial \hat{f}}{\partial z} = \sin \theta + \left(\frac{T}{w} \right) \frac{\partial \hat{\Phi}}{\partial \theta} . \quad (25)$$

In Eq. (25) \hat{f} is defined by

$$f_1 = \hat{f} \left(- \frac{w}{ZerB_0} \epsilon_t \right) \frac{\partial F_M}{\partial r} \frac{1}{\Omega_{th}} \left(\frac{v_c(w)}{\Omega_{th}} \right)^{-1/3} . \quad (26)$$

We note that when the dimensionless poloidal potential $\hat{\Phi} = O(1)$, it means that the contribution of the poloidal electric field to $\langle \dot{r} \rangle$ is of the same order as the magnetic drift contribution. Also, note that in Eq. (25) the kinetic energy w is a parameter, and the velocity space structure of \hat{f} is described through the dependence on z , which measures across the boundary layer around $\langle \dot{\theta} \rangle = 0$. Finally, we split Eq. (25) into its even and odd parts with respect to z , f^\pm :

$$\frac{\partial^2 f^+}{\partial z^2} - z \frac{\partial f^+}{\partial \theta} - y(w) \left[\sin \theta + \left(\frac{T}{w} \right) \frac{\partial \hat{\Phi}}{\partial \theta} \right] \frac{\partial f^-}{\partial z} = \sin \theta + \frac{T}{w} \frac{\partial \hat{\Phi}}{\partial \theta} , \quad (27)$$

$$\frac{\partial^2 f^-}{\partial z^2} - z \frac{\partial f^-}{\partial \theta} - y(w) \left[\sin \theta + \left(\frac{T}{w} \right) \frac{\partial \hat{\Phi}}{\partial \theta} \right] \frac{\partial f^+}{\partial z} = 0 . \quad (28)$$

These must be solved over the range $z \in [0, \infty)$, $\theta \in [-\pi, \pi]$. The boundary conditions at $z = 0$ are $\partial f^+ / \partial z(z = 0, \theta) = 0$, $f^-(z = 0, \theta) = 0$, and in the angle θ we impose periodicity $f^\pm(z, \theta = -\pi) = f^\pm(z, \theta = \pi)$. To determine the boundary conditions as $z \rightarrow \infty$, we return to Eq. (25) and observe that a particular solution is $-z/y$. Hence, if we write $\hat{f} = -z/y + \tilde{f}$ then \tilde{f} satisfies

$$\frac{\partial^2 \tilde{f}}{\partial z^2} - z \frac{\partial \tilde{f}}{\partial \theta} - y \left(\sin \theta + \frac{1}{x} \frac{\partial \hat{\phi}}{\partial \theta} \right) \frac{\partial \tilde{f}}{\partial z} = 0, \quad (29)$$

where $x = w/T$. If we now define

$$\omega = z^2 + 2y(\cos \theta - \hat{\phi}/x), \quad (30)$$

then Eq. (29) in the (ω, θ) space is

$$4 \frac{\partial}{\partial \omega} \left[z(\omega, \theta) \frac{\partial \hat{f}}{\partial \omega} \right] - \frac{\partial \hat{f}}{\partial \theta} = 0. \quad (31)$$

As $z \rightarrow \infty$ ($\omega \rightarrow \infty$) we expect that because all the velocity space structure occurs around $z = 0$, the second derivative term in Eq. (31) should be insignificant. If we expand Eq. (31) for large z in the smallness of the second derivative, we have, to lowest order, $\tilde{f} = \tilde{f}_0 = g(\omega)$. The function $g(\omega)$ can be determined from the next order,

$$4 \frac{\partial}{\partial \omega} \left(z \frac{\partial \tilde{f}_0}{\partial \omega} \right) - \frac{\partial \tilde{f}_1}{\partial \theta} = 0,$$

by requiring that \tilde{f}_1 be single-valued in Θ . This gives

$$\frac{dg}{d\omega} = \frac{\text{constant}}{\oint x(\omega, \theta) d\theta}.$$

The constant can be determined by requiring that $\partial \hat{f} / \partial z \rightarrow 0$ as $z \rightarrow \infty$ (that is, \hat{f} can be peaked around $z = 0$), and this gives the constant as π/y . Since $\partial / \partial \omega = (1/2z) \partial / \partial z$, we obtain, as $z \rightarrow \infty$, $\partial \tilde{f}_0 / \partial z \sim (2z)(\pi/y)(1/\oint z d\theta)$. We note that $\partial \tilde{f}_0 / \partial z$ is even in z ; hence $\tilde{f}_0 = \tilde{f}^-$, the odd part of \tilde{f} . When the particular solution is added back in, we obtain for f^-

$$\frac{\partial f^-}{\partial z}(z \rightarrow \infty, \theta) \sim -\frac{1}{y} + \frac{\pi}{y} \left(\frac{2z}{\oint z(\omega, \theta) d\theta} \right)_{\omega \approx z^2}. \quad (32)$$

The boundary condition for f^+ is obtained by noting that, for $z \rightarrow \infty$, \tilde{f}_1 must be even and hence $\hat{f}_1 = f^+$ (since z/y is odd). The solution for \tilde{f}_1 can be obtained from the constraint equation and gives

$$f^+(z \rightarrow \infty, \theta) \sim \frac{2\pi}{y} \left[\frac{1}{\oint z d\theta} \int^\theta \frac{1}{z} d\theta - \left(\oint \frac{1}{z} d\theta \right) \frac{1}{(\oint z d\theta)^2} \int^\theta z d\theta \right]_{\omega \approx z^2}, \quad (33)$$

where $\oint d\theta$ means $\int_{-\pi}^{\pi} d\theta$. We note that the boundary conditions involve the (as yet) unknown function $\hat{\psi}$. If one species (typically the ions) is in the low-collisionality superbanana regime, then in a single ion-electron plasma, where we can neglect the guiding center drifts of the electrons off the flux surface, the equation for $\hat{\psi}$ is, from Eq. (10),

$$n\epsilon_t \hat{\phi} \left(\frac{T_i}{T_e} + 1 \right) = \int \frac{dl}{B} \int d^3v f_1 \frac{1}{\int dl/B}, \quad (34)$$

where $n = \langle n_{0_i} \rangle = \langle n_{0_e} \rangle$, and f_1 is given by Eqs. (27) and (28) subject to the boundary conditions in Eqs. (32) and (33). In Eq. (34) we have averaged over a field line since the distribution function f_1 arises from the helically trapped particles, which are bouncing in the helical wells much faster than they are drifting off the flux surfaces.

This equation for $\hat{\phi}$ is a nonlinear differential equation since f_1 depends on $\partial \hat{\phi} / \partial \theta$ and $\hat{\phi}$ through the differential equation (25). We note that this arises from keeping the electrostatic contribution to $\langle \dot{r} \rangle_b$ in Eq. (25). In Ref. 1 this contribution was neglected in the kinetic equation, and this approximation was shown to be consistent because then $\hat{\phi} \propto \rho_{i_p} \partial \ln T_i / \partial r \ll 1$, where ρ_{i_p} is the poloidal ion gyroradius. If this approximation is made, Eq. (34) is a simple algebraic equation for $\hat{\phi}$. This approximation cannot be made for a stellarator or a bumpy torus since $\hat{\phi} \propto \sqrt{\epsilon_h / \epsilon_h} \partial \ln T_i / \partial r = O(1)$. For these nonaxisymmetric devices in the low-collisionality regime, the large orbit width¹¹ ($1/\epsilon_h$) as compared to the tokamak (ρ_{i_p}) makes $\hat{\phi}$ at least $O(1)$. We note that we can recover the functional form of the tokamak results of Ref. 1 by solving Eq. (25) with all the $\hat{\phi}$ terms dropped. This provides a useful means to validate the numerical code and illustrate the important differences between the tokamak and stellarator/bumpy torus cases. The velocity space integral in Eq. (34) is

$$\begin{aligned}
\int \frac{1}{dl/B} \int \frac{dl}{B} \int d^3v f_1 &= \frac{4\pi}{m_i^2} \int dw d\mu \int \frac{\tau_b}{dl/B} f_1 \\
&= \frac{4\pi}{m_i^2} \int dw \frac{2\tau_b}{|\partial\langle\dot{\theta}\rangle/\partial\mu|} \int \frac{1}{dl/B} \Omega_{th} \left(\frac{v}{\Omega_{th}}\right)^{1/3} \int_{-\infty}^{\infty} dz f_1 . \quad (35)
\end{aligned}$$

We use the magnetic field in Eq. (18) to obtain $\tau_b/\int dl/B = (2B_0/\pi)(m_i/w\epsilon_h)^{1/2}K(k)$. We approximate $|\partial\langle\dot{\theta}\rangle/\partial\mu|^{-1}$ in the limit where $\Omega_{E \times B} \ll \Omega_{th}$, where $\Omega_{E \times B}$ is the $\underline{E} \times \underline{B}$ azimuthal drift. Details can be found in Ref. 12. Then Eq. (34) becomes

$$\begin{aligned}
\hat{\Phi}(1 + T_i/T_e) &= -\frac{8(2.65)}{\sqrt{2}} \frac{\sqrt{\epsilon_h}}{\epsilon_h} \int_0^{\infty} \frac{dx x^{1/2}}{\pi^{3/2}} e^{-x} \left[\left(A_1 - \frac{5}{2}A_2 \right) \right. \\
&\quad \left. + xA_2 \right] \int_{-\infty}^{\infty} dz f^+(\hat{\Phi}, \partial\hat{\Phi}/\partial\theta) . \quad (36)
\end{aligned}$$

In Eq. (36) $\sqrt{\epsilon_h}$ is the fraction of helically trapped particles, $1/\epsilon_h$ is related to the orbit width, $A_1 = \partial \ln n/\partial r + \partial \ln T_i/\partial r + (\partial e\langle\dot{\Phi}\rangle/\partial r)/T_i$, $A_2 = \partial \ln T_i/\partial r$. The A_i are generalized forces arising from the spatial derivative of the Maxwellian. In the z integral, only the f^+ is kept since f^- will integrate to zero.

In order to complete the specification of $\hat{\Phi}$, we need to write $y(x)$ explicitly in terms of ϵ_t and ϵ_h . Along the resonance we can write

$$\Omega'_0 = -\frac{\epsilon_h^t}{\epsilon_h} \Omega_{E \times B} \lesssim -\frac{\epsilon_h^t}{\epsilon_h} |\Omega_{th}| . \quad (37)$$

This causes the function $y(x)$ to be

$$y(x) = \left[\frac{\Omega_{th}}{v(x)} \right]^{2/3} x \frac{\epsilon_h''}{(\epsilon_h')^2} \epsilon_t, \quad (38)$$

where we have used Eq. (37) to obtain Eq. (38) and $x = w/T$. The collision frequency evaluated along the resonance $\langle \dot{\theta} \rangle = 0$ is

$$\frac{v(x)}{\Omega_{th}} = \frac{m_i}{B_0} \left(\frac{v_D(x)}{\Omega_{th}} \right) \frac{\mu J}{\tau_b} \left[\frac{\partial}{\partial \mu} \left(\frac{\langle \dot{\theta} \rangle}{\Omega_{th}} \right) \right]^2 + \left(\frac{v_{||}(x)}{\Omega_{th}} \right) 2w^2 \left[\frac{\partial}{\partial w} \left(\frac{\langle \dot{\theta} \rangle}{\Omega_{th}} \right) \right]^2, \quad (39)$$

where $v_D(x)$ is the pitch-angle deflection frequency, $v_{||}(x)$ is the parallel velocity diffusion frequency, and $J = \int dl v_{||}$ is the second adiabatic invariant. We use the models $\epsilon_h = \epsilon_{h_0} r^2/a_p^2$, $\epsilon_t = \epsilon_{t_0} r/2a_p$. This gives

$$y(x) = \left(\frac{\epsilon_{t_0}}{\epsilon_{h_0}} \right) \left(\frac{v_{ii}}{\Omega_{th} \epsilon_{h_0}} \right)^{-2/3} x^{2/3} \left\{ (1.04) \left[1 + \operatorname{erf}(x^{1/2}) - G(x^{1/2}) \right] + 3.13 G(x^{1/2}) \right\}^{-2/3}, \quad (40)$$

where

$$G(p) = \frac{1}{2p^2} \left[\operatorname{erf}(p) - \frac{2pe^{-p^2}}{\sqrt{\pi}} \right]. \quad (41)$$

The dimensionless collisionality is $\hat{v} = [v_{ii}/(\epsilon_{h_0} \Omega_{th})]$, where v_{ii} is the ion-ion collision frequency evaluated at the thermal velocity. In

order for the particles to complete even the nonresonant orbits, we require $\hat{v} < 1$. In Eq. (25) the plasma is in the superbanana plateau regime when $y \ll 1$ [i.e., $v_{ii}/(\Omega_{th}\epsilon_t^{3/2})\sqrt{\epsilon_h} \gg 1$] and in the low-collisionality superbanana regime when $y \gg 1$ [i.e., $v_{ii}/(\Omega_{th}\epsilon_t^{3/2})\sqrt{\epsilon_h} \ll 1$].

In the superbanana plateau regime, $\hat{\Phi}$ can be obtained explicitly from Eqs. (25) and (36). This is because Eq. (25) with $y = 0$ can be solved exactly and the integral of f^+ over z performed analytically.¹² The result is

$$\begin{aligned} \bar{\Phi} & \left[-i \left(1 + \frac{T_i}{T_e} \right) - \frac{8(2.65)}{\epsilon_h} \frac{\sqrt{\epsilon_h}}{\sqrt{2}} \left(A_1 - 2A_2 \right) \right] \\ & \approx \frac{8(2.65)}{\epsilon_h} \frac{\sqrt{\epsilon_h}}{\sqrt{2}} \frac{i}{2} \left(A_1 - A_2 \right), \end{aligned} \quad (42)$$

where $\bar{\Phi}$ is defined by

$$\begin{aligned} \hat{\Phi} & = -\text{Re} \left[\frac{\bar{\Phi}}{i} e^{i\theta} \right] \\ & = -\text{Re}(\bar{\Phi}) \sin \theta - \text{Im}(\bar{\Phi}) \cos \theta. \end{aligned} \quad (43)$$

In Eq. (43) the first term on the left-hand side comes from the adiabatic contribution [see Eq. (7)] and the second term arises from the electrostatic contribution to the radial drift $\langle \dot{r} \rangle_b$, while the right-hand side arises from the magnetic drift contribution to $\langle \dot{r} \rangle_b$. Hence, we can clearly see in Eq. (43) that the self-consistent poloidal potential is driven by the magnetic drifts, a fact that came easily out of the Lagrangian approach in Sec. II. We can also recover the

functional form of $\hat{\phi}$ in the tokamak plateau regime.¹ If in Eq. (43) we neglect the electrostatic term on the left-hand side, we obtain

$$\hat{\phi} \propto \frac{1}{\epsilon_h'} (A_1 - A_2) \sin \theta, \quad (44)$$

whereas the tokamak plateau regime result is $\hat{\phi} \propto \rho_{ip} A_2 \sin \theta$. We see that in this limit the stellarator result is the same as the tokamak result with the replacement of the orbit width ρ_{ip} (the poloidal ion gyroradius) with $(\epsilon_h')^{-1}$. This type of poloidal potential will cause an up-down asymmetry in the potential contours. By contrast, if we include the self-consistent electrostatic contribution to the radial drift, and if it is larger than the adiabatic contribution (which it typically is because $\epsilon_h \ll 1$), then we obtain

$$\hat{\phi} \propto \left(\frac{A_1 - A_2}{A_1 - 2A_2} \right) \cos \theta. \quad (45)$$

We note that the parity in Eq. (45) is completely different from the expression in Eq. (46). This poloidal potential will give in-out asymmetry, not up-down asymmetry. In addition, we note that the potential is a rational function of the generalized forces (hence gradients). This will make the first-order distribution function a nonlinear function of the generalized forces and, therefore, make the fluxes nonlinear functions of the generalized forces. This interesting aspect of the poloidal potential was noted in Ref. 2. Its full consequences remain to be explored.

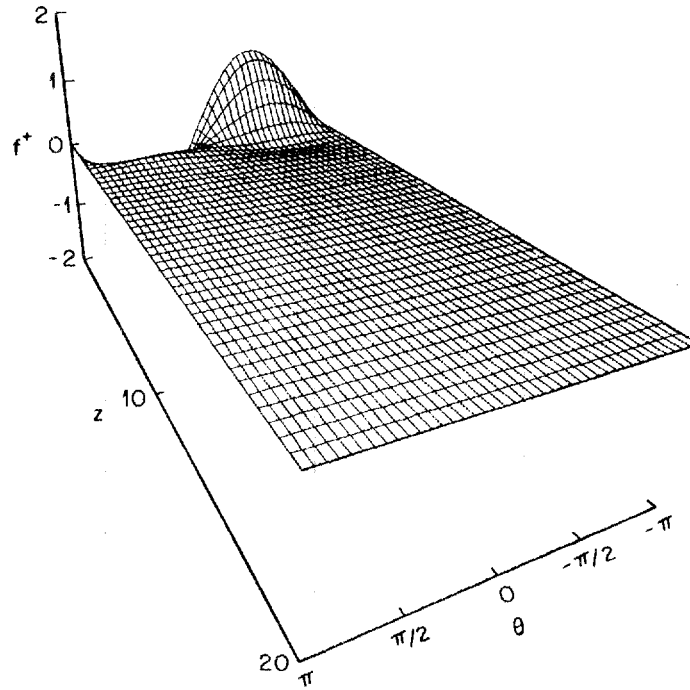
The simple form in Eq. (44) for the poloidal potential as a sine and cosine term is only obviously true in the superbanana plateau regime. For $y \geq 1$, it is easy to see from Eqs. (25) and (34) that if $\hat{\phi}$ is expanded in Fourier harmonics, there is no obvious reason to drop the higher harmonics. This is also clear from the tokamak banana result in Ref. 1, where they found $\hat{\phi} \propto \tan(\theta/2)$, which is not expressible as a sine and cosine term.

IV. DESCRIPTION OF THE NUMERICAL METHOD

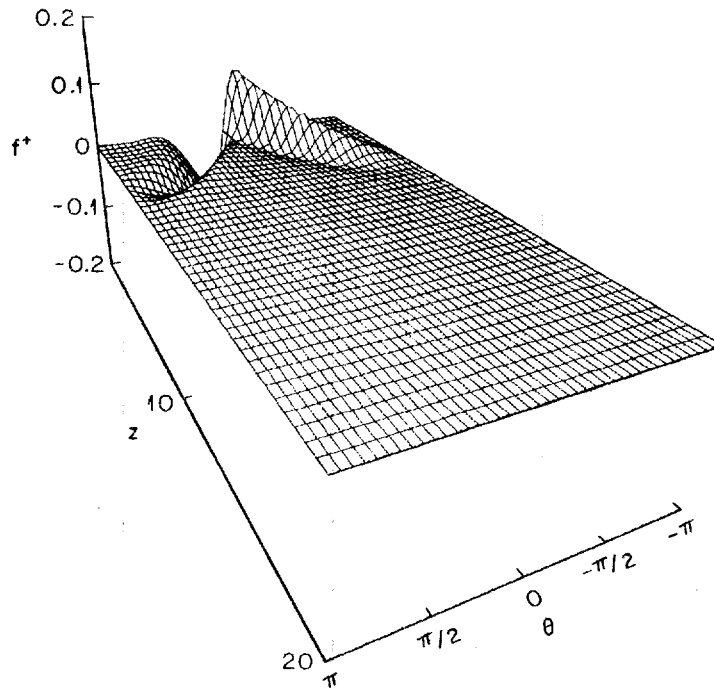
We have solved the kinetic equations [Eqs. (27) and (28)] over the range $z \in [0, \infty)$, $\theta \in [-\pi, \pi]$, subject to the boundary conditions in Eqs. (32) and (33) and using Eq. (40) for $y(x)$ and Eq. (36) for $\hat{\phi}(\theta)$. This has been done over a range of collisionalities $\hat{\nu}$.

The coupled equations [Eqs. (27) and (28)] were solved by finite differencing of the derivative terms and then by solving the coupled linear finite difference equations. Typically, 21 grid points were taken in the θ direction and 21 in the z direction. The outer value of z , z_{\max} , was typically chosen to be $z_{\max} = 20$. The code was designed to solve the equations with and without the $\partial\hat{\phi}/\partial\theta$ terms. If the $\partial\hat{\phi}/\partial\theta$ terms were to be turned off, the results should be the same functional form as obtained for a tokamak. Because the dimensionless energy, x , was a parameter in the equations, the equations were solved for a fixed value of x . This value of x was chosen to be $x = 1$ because this is where the energy integrand in Eq. (36) was peaked. In Fig. 1, we show a typical form for f^+ for $y \ll 1$, while in Fig. 2 we show a typical form for f^+ for $y \gg 1$. We can clearly see from these two figures that for $y \gg 1$, f^+ is much more highly peaked than for $y \ll 1$. As y

ORNL-DWG 85-2654 FED

Fig. 1. Distribution function f^+ for $y \ll 1$.

ORNL-DWG 85-2655 FED

Fig. 2. Distribution function f^+ for $y \gg 1$.

becomes larger and larger ($\hat{\nu} \rightarrow 0$), numerical difficulties result because the finite difference grid cannot resolve the peak. Unfortunately, we can only increase the number of grid points up to a point due to memory limitations on the computer. This effectively puts a lower limit on the value of $\hat{\nu}$ that can be considered. In practice, this turns out to be about $\hat{\nu} \approx 10^{-3}$.

Because the set of Eqs. (27), (28), and (36) is a coupled, nonlinear differential set for $\hat{\Phi}$, we have solved for $\hat{\Phi}$ by iteration. Unhappily, the straightforward iteration scheme suggested by Eq. (36) [that is, to evaluate $\hat{\Phi}$ on the left-hand side as the (n+1)th iteration if $\hat{\Phi}$ at the nth iteration is used inside f^+] is numerically unstable and so cannot be used at any $\hat{\nu}$ to find $\hat{\Phi}$. To circumvent this, Eq. (36) was coded as a set of nonlinear, coupled algebraic equations, and a root finder was called to solve the coupled algebraic equations.

Finally, once $\hat{\Phi}(\theta)$ was obtained, it was Fourier-analyzed and the Fourier coefficients were plotted as functions of collisionality $\hat{\nu}$.

V. NUMERICAL RESULTS

The numerical code was exercised in two ways. First, results were obtained with the $\partial\hat{\Phi}/\partial\theta$ terms in the kinetic equations (27) and (28) arbitrarily set to zero. This case corresponds to that of the tokamak, although only the functional form of $\hat{\Phi}(\theta)$ will be the same as the tokamak results, not the magnitude. We call these the "tokamak results" having the caveat just mentioned. Second, results were obtained for the stellarator/bumpy torus case with the $\partial\hat{\Phi}/\partial\theta$ terms fully included. For this case both the functional form and magnitude will be correct. We have called these results the "stellarator results."

In Fig. 3 we plot $\hat{\phi}(\theta)$ for the tokamak case for $\hat{v} = 1$. This corresponds to $y \ll 1$ and is in the plateau regime. As we expect, $\hat{\phi} \propto \sin \theta$. In Fig. 4 we plot $\hat{\phi}(\theta)$ for the tokamak case for $\hat{v} = 10^{-2}$. This corresponds to $y \gg 1$ and is deep in the banana regime. The result of Ref. 1 for this case is $\hat{\phi} \propto \cot(\theta/2)$. [They have $\tan(\theta/2)$, but our angle variable θ is shifted by π from theirs.] As was pointed out in Ref. 1, the result $\hat{\phi} \propto \cot(\theta/2)$ has a spurious singularity in it because the analytic treatment allows particles to spend an infinite amount of time at the banana tips. The numerical solution of the kinetic equations has no such problem and correctly includes the fact that particles near the banana tips are very likely to collide there and hence remove the singularity. We see this in Fig. 4, where the

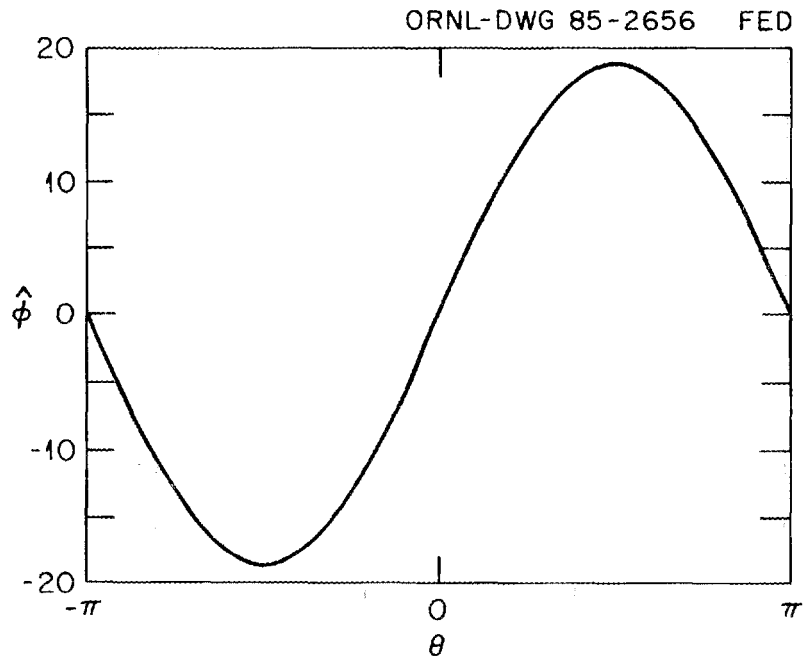


Fig. 3. Poloidal potential $\hat{\phi}(\theta)$ for $\hat{v} = 1$. Tokamak case.

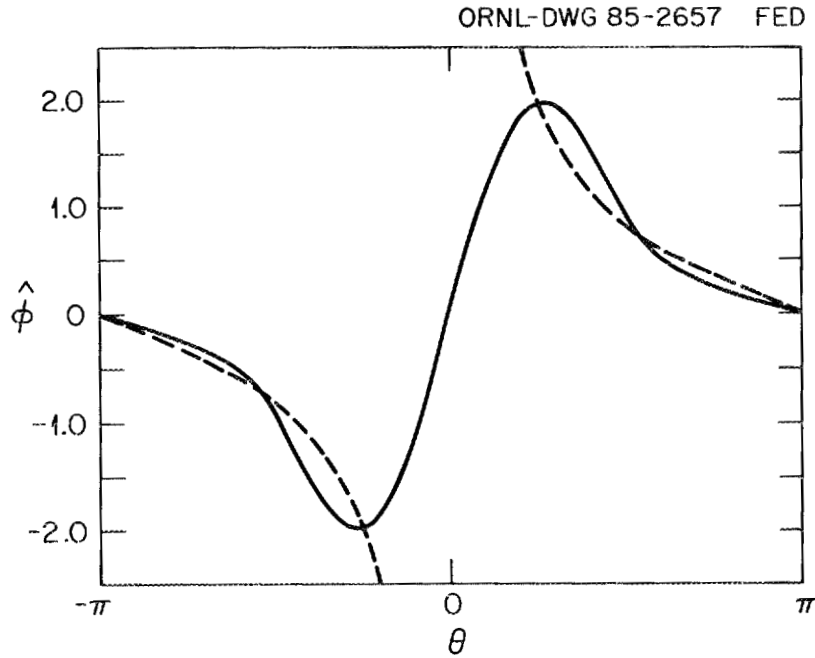


Fig. 4. Poloidal potential $\hat{\phi}(\theta)$ for $\hat{v} = 10^{-2}$. Tokamak case. Also plotted is the analytic result $\hat{\phi} \propto \cot(\theta/2)$.

$\cot(\theta/2)$ has a singularity at $\theta = 0$, but the numerical $\hat{\phi}$ matches $\cot(\theta/2)$ away from $\theta = 0$ but remains finite at $\theta = 0$.

In Fig. 5 we Fourier decompose $\hat{\phi}$ as

$$\hat{\phi} = \sum_{n=1}^{\infty} a_n \cos n\theta + b_n \sin n\theta$$

and plot a_n/\hat{v} and b_n/\hat{v} against \hat{v} for $n = 1, \dots, 5$. Because in the plateau regime the distribution function is independent of \hat{v} and in the banana regime it varies linearly with \hat{v} , we expect to find $\hat{\phi} \propto \hat{v}$ in the banana regime and $\hat{\phi}$ independent of \hat{v} in the plateau regime. This fact is borne out by the analytic results of Ref. 1. In the banana regime,

the dependence of $\hat{\Phi}$ on $\hat{\nu}$ arises because the collisions break the symmetry of the orbits. The collisionless orbits cannot directly make a contribution to $\hat{\Phi}$ because the orbit deviation is symmetric about the flux surface and hence gives zero net effect. If $\hat{\Phi} \propto \hat{\nu}$ for $\hat{\nu} \ll 1$, then $\hat{\Phi}/\hat{\nu}$ should be a constant for small $\hat{\nu}$, and for $\hat{\nu} \approx 1$ we expect $\hat{\Phi}/\hat{\nu} \propto 1/\hat{\nu}$. In Fig. 5 we see that at $\hat{\nu} = 1$ there is only a b_1 term corresponding to the $\sin \theta$ component of $\hat{\Phi}$ previously mentioned. As $\hat{\nu}$ decreases, $b_2/\hat{\nu}$, $b_3/\hat{\nu}$, and $b_5/\hat{\nu}$ start to appear and go to constants, indicating that for $\hat{\nu} \ll 1$, $\hat{\Phi} \propto \hat{\nu}$. We note that none of the a_n 's ever appear in significant proportions, indicating that the poloidal potential maintains its up-down asymmetry over this range of collisionality but has no in-out asymmetry. We can also clearly see the point made in Sec. III that, for $\hat{\nu} \rightarrow 0$, more and more Fourier

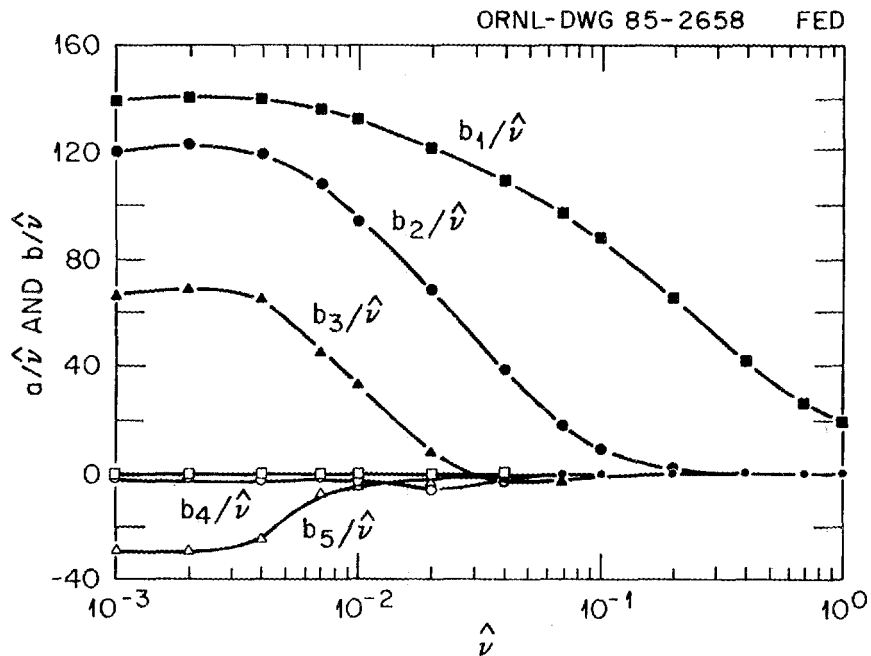


Fig. 5. Fourier components of $\hat{\Phi}/\hat{\nu}$ against $\hat{\nu}$. Tokamak case.

harmonics are excited. This arises from the banana shape of the orbits.

In Fig. 6 we plot $\hat{\phi}(\theta)$ for $\hat{\nu} = 1$ for the stellarator case. We see the cosine dependence as we would expect since $y \ll 1$. We note that $\hat{\phi} = O(1)$, which indicates that the electrostatic effect in $\langle \dot{r} \rangle_b$ is just as important as the magnetic effect. In Fig. 7 we plot $\hat{\phi}(\theta)$ for $\hat{\nu} = 10^{-2}$ for the stellarator case. In contrast to the tokamak case, $\hat{\phi}(\theta)$ looks just like the result for $\hat{\nu} = 1$. This is confirmed in Fig. 8, where we plot the Fourier components of $\hat{\phi}(\theta)$ against $\hat{\nu}$ for the stellarator case. We see that all the b_n 's remain very small, and the only a_n component that appears is a_1 , which is almost a constant. Hence, we find the remarkable result that, at least over the range of collisionalities shown here, for a stellarator or bumpy torus the poloidal potential retains the simple form of the plateau regime well

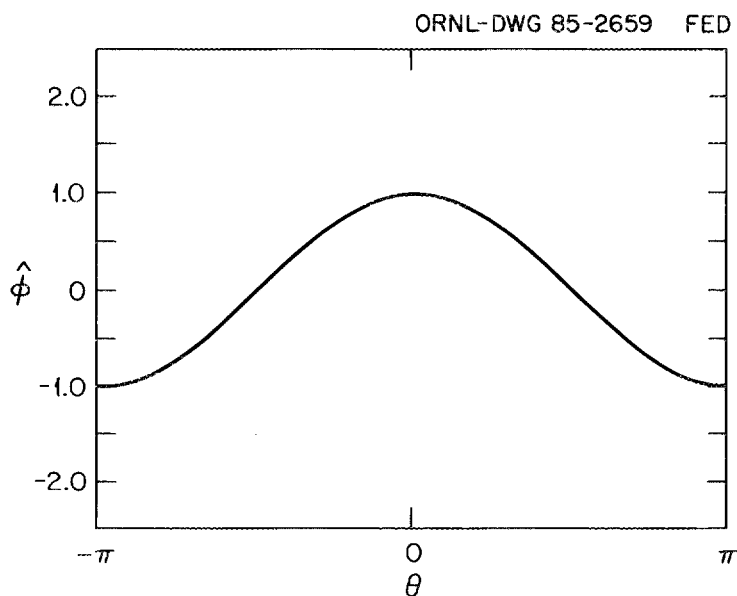


Fig. 6. Poloidal potential $\hat{\phi}(\theta)$ for $\hat{\nu} = 1$. Stellarator case.

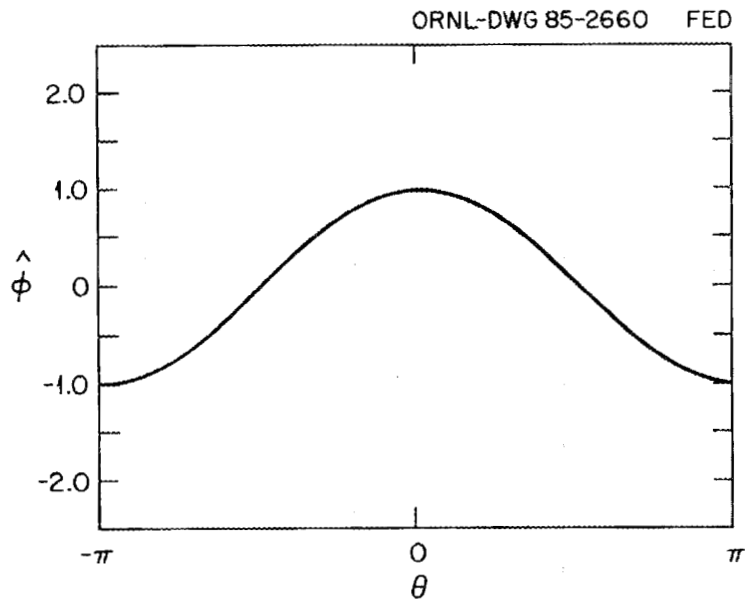


Fig. 7. Poloidal potential $\hat{\phi}(\theta)$ for $\hat{\nu} = 10^{-2}$. Stellarator case.

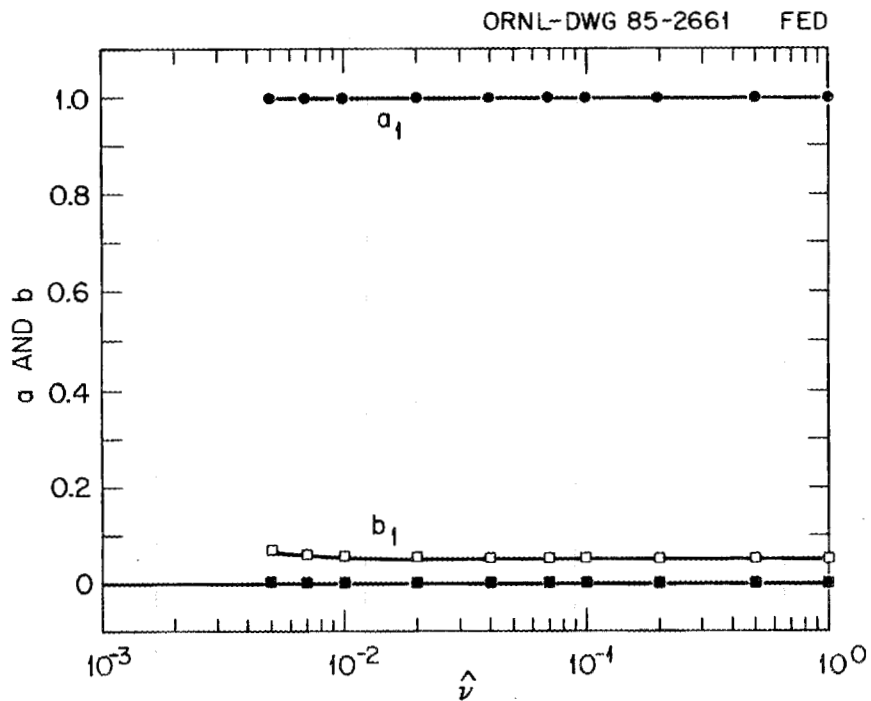


Fig. 8. Fourier components of $\hat{\phi}$ against $\hat{\nu}$. Stellarator case.

into the banana regime. We note also that the poloidal potential is only very weakly dependent on the collisionality, in strong contrast to the tokamak case. The reason for this remarkable behavior can be understood by noting that if $\hat{\phi} \propto \cos \theta$ in Eq. (30), then this corresponds to a simple shift in the parameter y so as to reduce it. Hence, when the $\partial\hat{\phi}/\partial\theta$ term is retained in the kinetic equations, the particles in the plateau regime continue to make most of the contribution to the integrals in Eq. (36). Therefore, the poloidal potential retains the plateau functional form and magnitude deep into the superbanana regime. This interesting result means that the potential contours, even deep into the banana regime in the stellarator, will be circular with an in-out asymmetry. In contrast, in the tokamak case, the potential contours will be up-down asymmetric and possess significant amounts of ellipticity, triangularity, and D-shaping.

VI. CONCLUSIONS

We have defined the problem of calculating the poloidal potential for a stellarator or bumpy torus in the low-collisionality superbanana regime. The potential is coupled to the kinetic equation for the first-order distribution function, which gives the potential. This nonlinear differential set of equations was solved numerically. For the tokamak case, the numerical results confirmed the analytic work and indicated significant structure to the poloidal potential in the banana regime. For the stellarator/bumpy torus case, the numerical results indicated that the poloidal potential continues to look like the plateau result even into the banana regime. Hence for the stellarator,

the structure of the potential remains very simple even into the banana regime.

Future research should include the consideration of the poloidal potential in a stellarator having impurities and other physical effects that have been found in tokamaks to affect the potential. This numerical work indicates that, for the purpose of calculation, the electrostatic contribution to $\langle r \rangle_b$ has the same magnitude and form as the magnetic contribution. This greatly simplifies numerical transport simulations.

ACKNOWLEDGMENTS

The authors would like to acknowledge useful discussions with Prof. Herb Berk, Prof. Kim Molvig, and with Dr. John Whitson, who provided useful numerical guidance.

This research was sponsored by the Office of Fusion Energy, U.S. Department of Energy, under Contract No. DE-AC05-OR21400.

REFERENCES

- ¹F. L. Hinton and M. N. Rosenbluth, Phys. Fluids 16, 836 (1973).
- ²R. D. Hazeltine and A. A. Ware, Phys. Fluids 19, 1163 (1976).
- ³C. S. Chang, Phys. Fluids 26, 2140 (1983).
- ⁴J. Y. Hsu, G.A. Technologies Report GA-A17474 (1984).
- ⁵D. E. Hastings, Phys. Fluids 27, 2272 (1984).
- ⁶X. S. Lee, J. R. Myra, and P. J. Catto, Phys. Fluids 27, 2248 (1984).
- ⁷H. Mynick, Phys. Fluids 27, 2086 (1984).
- ⁸A. El-Nadi, Phys. Fluids 28, 878 (1985).
- ⁹I. B. Bernstein and K. Molvig, Phys. Fluids 26, 1488 (1983).
- ¹⁰D. E. Hastings, E. F. Jaeger, C. L. Hedrick, and J. S. Tolliver, Phys. Fluids 26, 1516 (1983).
- ¹¹R. D. Hazeltine and P. J. Catto, Phys. Fluids 24, 920 (1981).
- ¹²D. E. Hastings and K. C. Shaing, Phys. Fluids 28, 1402 (1985).

INTERNAL DISTRIBUTION

- | | |
|----------------------|--------------------------------------|
| 1. F. W. Baity | 15. J. B. Wilgen |
| 2. B. A. Carreras | 16-17. Laboratory Records Department |
| 3. R. A. Dory | 18. Laboratory Records, ORNL-RC |
| 4. J. C. Glowienka | 19. Document Reference Section |
| 5. G. R. Haste | 20. Central Research Library |
| 6. D. L. Hillis | 21. Fusion Energy Division Library |
| 7. J. Sheffield | 22-23. Fusion Energy Division |
| 8. D. A. Spong | Publications Office |
| 9-13. J. S. Tolliver | 24. ORNL Patent Office |
| 14. T. Uekan | |

EXTERNAL DISTRIBUTION

- 25-29. D. E. Hastings, Massachusetts Institute of Technology, 77 Massachusetts Avenue, Cambridge, MA 02139
30. J. F. Clarke, Associate Director of Fusion Energy, Office of Fusion Energy, Office of Energy Research, ER-50, Germantown, U.S. Department of Energy, Washington, DC 20545
31. D. B. Nelson, Director, Division of Applied Plasma Physics, Office of Fusion Energy, Office of Energy Research, ER-54, Germantown, U.S. Department of Energy, Washington, DC 20545
32. M. N. Rosenbluth, RLM 11.218, Institute for Fusion Studies, University of Texas, Austin, TX 78712
33. W. Sadowski, Fusion Theory and Computer Services Branch, Office of Fusion Energy, Office of Energy Research, ER-541, Germantown, U.S. Department of Energy, Washington, DC 20545
34. A. Opdenaker, Fusion Systems Design Branch, Division of Development and Technology, Office of Fusion Energy, Office of Energy Research, ER-532, Germantown, U.S. Department of Energy, Washington, DC 20545
35. P. M. Stone, Fusion Systems Design Branch, Division of Development and Technology, Office of Fusion Energy, Office of Energy Research, ER-532, Germantown, U.S. Department of Energy, Washington, DC 20545
36. J. M. Turner, International Programs, Office of Fusion Energy, Office of Energy Research, ER-52, Germantown, U.S. Department of Energy, Washington, DC 20545
37. N. A. Davies, Office of the Associate Director, Office of Fusion Energy, Office of Energy Research, ER-51, Germantown, U.S. Department of Energy, Washington, DC 20545
38. E. Oktay, Division of Confinement Systems, Office of Fusion Energy, Office of Energy Research, ER-55, Germantown, U.S. Department of Energy, Washington, DC 20545
39. Theory Department Read File, c/o D. W. Ross, Institute for Fusion Studies, University of Texas at Austin, RLM 11.222, Austin, TX 78712
40. Theory Department Read File, c/o R. C. Davidson, Director, Plasma Fusion Center, 167 Albany Street, Cambridge, MA 02139

41. Theory Department Read File, c/o F. W. Perkins, Princeton Plasma Physics Laboratory, P.O. Box 451, Princeton, NJ 08544
42. Theory Department Read File, c/o L. Kovrizhnykh, Institute of General Physics, U.S.S.R. Academy of Sciences, Ulitsa Vavilova, 38, Moscow, U.S.S.R. V312
43. Theory Department Read File, c/o B. B. Kadomtsev, I. V. Kurchatov Institute of Atomic Energy, P.O. Box 3402, Moscow, U.S.S.R. 123182
44. Theory Department Read File, c/o T. Kamimura, Institute of Plasma Physics, Nagoya University, Nagoya, Japan
45. Theory Department Read File, c/o C. Mercier, Euratom-CEA, Service de Recherches sur la Fusion Controlee, Fontenay-aux-Roses (Seine), France
46. Theory Department Read File, c/o T. E. Stringer, JET Joint Undertaking, Culham Laboratory, Abingdon, Oxfordshire, OX14 3DB, England
47. Theory Department Read File, c/o K. Roberts, Culham Laboratory, Abingdon, Oxon, OX14 3DB, England
48. Theory Department Read File, c/o D. Biskamp, Max-Planck Institut fur Plasmaphysik, D-8046 Garching bei Munchen, Federal Republic of Germany
49. Theory Department Read File, c/o T. Takeda, Japan Atomic Energy Research Institute, Tokai, Naka, Ibaraki, Japan
50. Theory Department Read File, c/o C. S. Liu, GA Technologies, Inc., P.O. Box 81608, San Diego, CA 92138
51. Theory Department Read File, c/o L. D. Pearlstein, L-630, Lawrence Livermore National Laboratory, P.O. Box 5511, Livermore, CA 94550
52. Theory Department Read File, c/o R. A. Gerwin, CTR Division, M-F642, Los Alamos National Laboratory, P.O. Box 1663, Los Alamos, NM 87545
53. R. E. Mickens, Atlanta University, Department of Physics, Atlanta, GA 30314
54. G. Swanson, Auburn University, Auburn, AL 36849
55. Office of the Assistant Manager for Energy Research and Development, U.S. Department of Energy, Oak Ridge Operations, Box E, Oak Ridge, TN 37831
56. J. D. Callen, Department of Nuclear Engineering, University of Wisconsin, Madison, WI 53706
57. R. W. Conn, Department of Chemical, Nuclear, and Thermal Engineering, University of California, Los Angeles, CA 90024
58. S. O. Dean, Director, Fusion Energy Development, Science Applications International Corporation, 2 Professional Drive, Suite 249, Gaithersburg, MD 20879
59. H. K. Forsen, Bechtel Group, Inc., Research Engineering, P.O. Box 3965, San Francisco, CA 94105
60. J. R. Gilleland, GA Technologies, Inc., Fusion and Advanced Technology, P.O. Box 81608, San Diego, CA 92138
61. R. W. Gould, Department of Applied Physics, California Institute of Technology, Pasadena, CA 91125
62. R. A. Gross, Plasma Research Laboratory, Columbia University, New York, NY 10027
63. D. M. Meade, Princeton Plasma Physics Laboratory, P.O. Box 451, Princeton, NJ 08544
64. W. M. Stacey, School of Nuclear Engineering, Georgia Institute of Technology, Atlanta, GA 30332
65. D. Steiner, Rensselaer Polytechnic Institute, Nuclear Engineering Department, NES Building, Tibbets Avenue, Troy, NY 12181
66. R. Varma, Physical Research Laboratory, Navrangpura, Ahmedabad 380009, India
67. Bibliothek, Max-Planck Institut fur Plasmaphysik, D-8046 Garching, Federal Republic of Germany
68. Bibliothek, Institut fur Plasmaphysik, KFA, Postfach 1913, D-5170 Julich, Federal Republic of Germany

69. Bibliotheque, Centre de Recherches en Physique des Plasmas, 21 Avenue des Bains, 1007 Lausanne, Switzerland
70. Bibliotheque, Service du Confinement des Plasma, CEA, B.P. 6, 92 Fontenay- aux-Roses (Seine), France
71. Documentation S.I.G.N., Departement de la Physique du Plasma et de la Fusion Controlee, Centre d'Etudes Nucleaires, B.P. No. 85, Centre du Tri, 38041 Cedex, Grenoble, France
72. Library, Culham Laboratory, UKAEA, Abingdon, Oxfordshire, OX14 3DB, England
73. Library, FOM Instituut voor Plasma-Fysica, Rijnhuizen, Jutphaas, The Netherlands
74. Library, Institute of Plasma Physics, Nagoya University, Nagoya 464, Japan
75. Library, International Centre for Theoretical Physics, Trieste, Italy
76. Library, Laboratorio Gas Ionizzati, Frascati, Italy
77. Library, Plasma Physics Laboratory, Kyoto University, Gokasho, Uji, Kyoto, Japan
78. Plasma Research Laboratory, Australian National University, P.O. Box 4, Canberra, A.C.T. 2000, Australia
79. Thermonuclear Library, Japan Atomic Energy Research Institute, Tokai, Naka, Ibaraki, Japan
- 80-235. Given distribution as shown in TIC-4500 Magnetic Fusion Energy (Category Distribution UC-20 g: Theoretical Plasma Physics)